

**XVI-th International Symposium on  
Electrical Apparatus and Technologies**



**SIELA 2009**

**PROCEEDINGS**

**Volume II**

---

**4–6 June 2009  
Bourgas, Bulgaria**

---



**ELKABEL**

Union of Electronics, Electrical Engineering and Telecommunications (CEECE)  
Federation of Scientific and Technical Unions  
Technical Universities of Sofia, Varna and Gabrovo  
State Agency for Information Technologies and Communications  
University of Mining and Geology "St. Ivan Rilski"  
Ruse University „Angel Kantchev"  
Bourgas Free University  
Houses of Science and Technology – Plovdiv, Bourgas, Varna and Montana

**XVI-th International Symposium on Electrical  
Apparatus and Technologies**

**SIELA 2009**



**PROCEEDINGS**  
**Volume II**

**4 – 6 June 2009**  
**Bourgas, Bulgaria**

**ISBN 978-954-323-560-5**

## Programme Committee

**Chairman:** Ivan YATCHEV, Bulgaria

### Members:

Slavoljub ALEKSIC, Serbia  
 Alexander ALEXANDROV, Bulgaria  
 Gancho BOJLOV, Bulgaria  
 Grigore CIVIDJIAN, Romania  
 Dimitar DIMITROV, Bulgaria  
 Peter DINEFF, Bulgaria  
 Gerhard DREGER, Germany  
 Bülent ERTAN, Turkey  
 Bernd FRANKE, Germany  
 Laurent GERBAUD, France  
 Leonid GRCEV, Macedonia  
 Kemal HOT, Croatia  
 Wilfried JAEGER, Germany  
 Tapani JOKINEN, Finland  
 Yasushi KANAI, Japan  
 Antonios KLADAS, Greece  
 Christian MAGELE, Austria  
 Iliana MARINOVA, Bulgaria  
 Ivan MASLAROV, Bulgaria  
 Bogdan MIEDZINSKI, Poland  
 Michel POLOUJADOFF, France  
 Ioan POPA, Romania  
 Oleg PUULO, Ukraine  
 Maurizio REPETTO, Italy  
 Maxim RIABCHITSKY, Russia  
 Ewen RITCHIE, Denmark  
 Yuri ROZANOV, Russia  
 Marek RUDNICKI, Poland  
 Yoshifuru SAITO, Japan  
 Vladimir SHEVCHENKO, Ukraine  
 Iliana STANEV, Bulgaria  
 Emil SOKOLOV, Bulgaria  
 Jan STROJNY, Poland  
 Jan SYKULSKI, England  
 Dimitar YUDOV, Bulgaria  
 Hans-Heinz ZIMMER, Germany  
 Sergey ZIRKA, Ukraine

## CONTENTS

<i>Michael JAINDL, Alice KÖSTINGER, Christian MAGELE and Werner RENHART</i>	Austria	
<b>Multi-objective optimization using evolution strategies</b> .....		7
<i>Zlata CVETKOVIĆ, Bojana PETKOVIĆ, Mirjana PERIĆ</i>	Serbia	
<b>An external body in protected area</b> .....		23
<i>Peter DINEFF, Dilyana GOSPODINOVA, Ivalina ABRAMOVA</i>	Bulgaria	
<b>Energy characteristics and parameters of non-uniform (pin-to-plane) dielectric barrier discharge</b> .....		30
<i>Peter DINEFF, Dilyana GOSPODINOVA, Momchil SHOPOV</i>	Bulgaria	
<b>Non-equilibrium air discharge device for plasma-chemical functionalization</b> .....		40
<i>Elissaveta GADJEVA and Nikolay GADZHEV</i>	Bulgaria	
<b>A nullator-norator model-based approach to analog circuit diagnosis</b> .....		50
<i>Elissaveta GADJEVA and Vladislav DUREV</i>	Bulgaria	
<b>Application of parametric spice simulation to hbt small-signal model parameter extraction</b> .....		58
<i>Georgi GANEV, Ekaterina GUEORDJEVA</i>	Bulgaria	
<b>An approach to estimation of low power loads influence on the supply grid</b> .....		66
<i>Georgi GANEV</i>	Bulgaria	
<b>Non-linear low power loads influence on the neutral current</b> .....		74
<i>Georgi GANEV, George TODOROV, A.KASSAMAKOV</i>	Bulgaria	
<b>Three-phase transformer additional losses</b> .....		82
<i>Galia GEORGIEVA-TASKOVA, Iliana MARINOVA, Valentin MATEEV</i>	Bulgaria	
<b>Electric field distribution of high pressure discharge lamps</b> .....		88
<i>Galia GEORGIEVA-TASKOVA, Iliana MARINOVA, Valentin MATEEV</i>	Bulgaria	
<b>Thermal modelling of high pressure discharge lamps</b> .....		95
<i>Zaharinka GERGOVA, Vultchan GUEORGIEV, Ivan YATCHEV and Alexander ALEXANDROV</i>	Bulgaria	
<b>Influence of some physical factors on the inductance of a coil with straight ferromagnetic core</b> .....		103
<i>Vultchan GUEORGIEV</i>	Bulgaria	
<b>Some aspects of heating analysis of electrical equipment</b> .....		109
<i>Vultchan GUEORGIEV, Krastio HINOV and Ivan YATCHEV</i>	Bulgaria	
<b>Static force characteristics of a permanent magnet electromagnetic valve actuator - 3d finite element modelling and experiment</b> .....		115
<i>Vultchan GUEORGIEV, Nikolaj MATANOV, Borislav BOJCHEV, Vasil GOSPODINOV</i>	Bulgaria	
<b>Energy efficiency of different approaches for compensation of capacitive loads</b> .....		123

<i>Ilona IATCHEVA, Rumena STANCHEVA, Hristofor TAHRILOV and Ilonka LILIANOVA</i>	Bulgaria	
<b>Theoretical and experimental investigations of induction heating system</b> .....		130
<i>Ozan KEYSAN, H. Bülent ERTAN</i>	Turkey	
<b>Determination of rotor slot number of an induction motor using an external search coil</b> ....		141
<i>Kostadin KOSTADINOV, Chavdar ALEXANDROV, Miroslav TSVETKOV</i>	Bulgaria	
<b>Applications of TCP/IP based radar-computer interface</b> .....		149
<i>Vladimir LAZAROV, Daniel ROYE, Zahari ZARKOV and Dimitar SPIROV</i>	Bulgaria, France	
<b>Analysis of DC converters for wind generators</b> .....		157
<i>Dian MALAMOV, Stanimira SHISHKOVA-PANAYOTOVA</i>	Bulgaria	
<b>Heating the socket-joints of a contact system with parallel branches</b> .....		165
<i>Iliana MARINOVA and Valentin MATEEV</i>	Bulgaria	
<b>3D model building of anatomical objects</b> .....		172
<i>Iliana MARINOVA and Valentin MATEEV</i>	Bulgaria	
<b>Modeling of electromagnetic fields in human tissue objects</b> .....		178
<i>Iliana MARINOVA and Valentin MATEEV</i>	Bulgaria	
<b>Electromagnetic interactions in medical applications</b> .....		184
<i>Valentin MATEEV</i>	Bulgaria	
<b>Computer system for electromagnetic property measurements of biological objects</b> .....		192
<i>Bogdan MIEDZINSKI, Marcin HABRYCH, Zenon OKRASZEWSKI, Xin WANG, LJ XU</i>	Poland, China	
<b>Efficiency of the 3-phase system to provide energy under low frequency induction heating of CWRs</b> .....		199
<i>Kostadin MILANOV, Mihaela SLAVKOVA and Mintcho MINTCHEV</i>	Bulgaria	
<b>A study of inrush currents in PWM converters under frequently electrical mains interruptions</b> .		207
<i>Kostadin MILANOV, Mihaela SLAVKOVA</i>	Bulgaria	
<b>Survey of requirements to permanent magnets</b> .....		213
<i>Ivan MILENOV, Krasimir KRASTANOV, Chavdar DZHAMBASKI</i>	Bulgaria	
<b>A study on joint operation of super capacitors and storage batteries</b> .....		221
<i>Ana MLADENOVIĆ and Slavoljub ALEKSIĆ</i>	Serbia	
<b>Magnetic field determination of block permanent magnet magnetized in arbitrary direction</b> .....		228
<i>Nebojša RAIČEVIĆ, Saša ILIĆ, Slavoljub ALEKSIĆ</i>	Serbia	
<b>Refractive modelling of electric field at cable termination</b> .....		235
<i>Jordan SHOPOV, Simona PETRAKIEVA</i>	Bulgaria	
<b>Phase control in the primary circuit of the power transformers</b> .....		243
<i>Dragana ŽIVALJEVIĆ, Vidosav STOJANOVIĆ</i>	Serbia	
<b>Complementary IIR filter synthesis without transformation variable</b> .....		251

# ENERGY CHARACTERISTICS AND PARAMETERS OF NON-UNIFORM (PIN-TO-PLANE) DIELECTRIC BARRIER DISCHARGE

Peter DINEFF\*, Dilyana GOSPODINOVA\*, Ivalina ABRAMOVA\*\*

\*Technical University of Sofia, Department of Electrical Apparatus, 1156 Sofia, 8, St. Kliment Ohridski, Bulgaria, E-mail: [dineff\\_pd@abv.bg](mailto:dineff_pd@abv.bg); [dilianang@abv.bg](mailto:dilianang@abv.bg)

\*\*Institute of General and Inorganic Chemistry, Bulgarian Academy of Sciences, 1113 Sofia, 11, Acad. Georgi Bonchev" str.; E-mail: [iva@svr.igic.bas.bg](mailto:iva@svr.igic.bas.bg)

**Abstract.** Interesting types of DBD in ambient air at atmospheric pressure for the generation of non-thermal plasma on dielectric surfaces were investigated. *Pin-to-plane dielectric barrier discharge* was sustained in the electrode configurations combining electrode components of both corona and DBD – metallic pins or triangle spikes electrode, situated single- or double-in-line and metallic plate electrode covered with a dielectric barrier. It was investigated experimentally the burning mode of this new discharge in ambient air. The discharge behavior with single- and double-in-line spikes high voltage electrode was discussed. The *pin-to-plane DBD* is a new DBD-based discharge rich in energy that produces a lot of chemically active centers on the wood surface by functionalization (oxidation).

**Keywords:** burning voltage, critical parameters, dielectric barrier discharge, non-uniformity, operating area, single- and double-in-line spike electrode.

## INTRODUCTION

The surface properties are determined by a thin layer of molecular dimensions and can be changed without influencing the bulk properties of the low surface energy materials. Paper, fibers and other cellulosic materials are mostly characterized by non-polar chemically inert surfaces with surface energy in the 20-40 mN/m range. In general, wood (cellulosic) materials are wetted by liquids when the surface energy of the wood surface exceeds the surface energy of the liquid. The surface energy of common organic solvent is lower than that of the wood, therefore paints, inks, adhesive and impregnating solution based on organic solvents are successfully applied to wood and cellulosic materials. Environmental requirements call for a replacement by water-based paints, inks and bonding agents. Flame retardancy is accomplished by capillary impregnation with water solution containing different kind of flame retardants. Because of the high surface tension of water (72.1 mN/m) a treatment of low energy surface is necessary to improve their surface energy.

Low surface energy impedes surface contamination and allows easy cleaning, but it complicates such processing as printing, coating, sticking, impregnation, etc. Various processes have been developed for surface treatment to enhance adhesion and capillary activity, such as mechanical treatment, wet-chemical treatment, exposure to flames, and cold (non-thermal) plasma treatment in atmospheric dielectric barrier discharge (*A-DBD*).

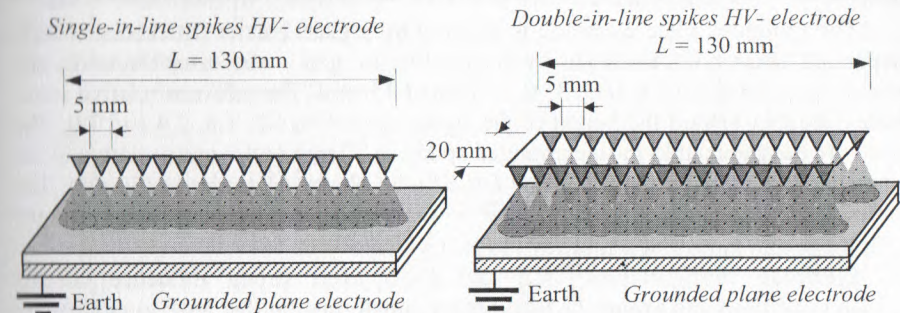


**Figure 1.** Electrode configurations of dielectric barrier discharge (DBD): **a** – *pin-to-plane DBD* with *single-in-line* spikes electrode (*SILS* electrode); **b** – *pin-to-plane DBD* with *double-in-line* spikes electrode (*SILS* electrode).

Plasma surface treatment of dielectric surfaces at atmospheric pressure with *alternative current barrier corona (AC-BC)* or *pin-to-plane DBD* were published recently (Akishev et al, 2002; Radu et al, 2003). These discharges were sustained in the electrode configuration combining the electrode elements of both:– a pins (spike) electrode came from corona discharge, and a plate electrode covered with a dielectric barrier came from *A-DBD*. The authors experimentally and theoretically investigated the burning mode of this *pin-to-plane DBD* in ambient air at atmospheric pressure. Diverse applications including the functionalization demand a solid physical and chemical understanding of the operational principals of such discharges.

The effect of plasma surface treatment and pre-treatment depends on the energy input into the plasma-chemical surface (or volume) process. For the energy flow on a resting substrate surface, the dosage  $D$  is used:  $D = (P t) / A$ , (W sek)/m<sup>2</sup> or J/m<sup>2</sup>, where  $P$  is the real power introduced into the discharge, W;  $A$  is the substrate (electrode) surface, m<sup>2</sup>; and  $t$  is the process duration of the, sek. If the substrate surface is moving with linear velocity  $\vartheta$ , m/sek, for the absorbed energy flow the dosage  $D$  is used:  $D = P / (b \vartheta)$ , J/m<sup>2</sup>, where  $b$  is the treated surface width, m. The real power  $P$  introduced into the discharge is an important parameter to achieve desired surface chemistry for the both surface material operations and it characterize the result of the chemical interaction of non-thermal plasma with the low energy treated surface.

The aim of this paper is the experimental study of energy characteristics and parameters of a special *pin-to-plane DBD* with different electrode configuration, Fig. 1.

## EXPERIMENTAL INVESTIGATION

The *pin-to-plate DBDs* are typical discharges with expressed local non-uniformity closeness high-voltage electrode that consists a lot of pins (spikes) arranged the length of electrode according two way – *single-in-line* or *double-in-line*, Fig. 1a and b. An alumina profile is used for making the two studded high voltage electrode configurations with *single-in-line (SIL)* and *double-in-line (DIL)* arranged spikes, Fig. 1.

The grounded plate electrode is covered by a glass barrier (thickness: 3 mm) and separated form high electrode by a variable air gap – the inter-electrode gap distance  $d$  is varies on five levels: 3, 6, 9, 12 and 15 mm. The relevant relative inter-electrode distances toward the height of the spikes are – 0.6, 1.2, 1.8, 2.4 and 3.0. The distance between the double-in-line arranged spikes is 20 mm or 4.0 units relative to the spike height. The length of the *SILS-* and *DILS* high voltage electrodes is 130 mm. The electrodes are energized by a high voltage power supply with typical voltages in the 1+20 kV range and industrial frequency (50 Hz), [1, 2].

Electrode configurations *SILS* and *DILS* exert strong influence on the breakdown conditions and avalanche to streamer transformation that have to modify not only the *DBD*'s volt-ampere characteristic, ignition  $U_b$  voltage, and critical parameters of operating sub-area, [1], but the energy effectiveness operational parameters of the operational (real power-voltage) characteristics -  $P = \varphi(U_{RMS}), d = const.$

The static volt-ampere characteristics of *pin-to-plane DBDs* have been plotted experimentally, linear polygonal discharge models have been worked out in accordance with a well known method for a minimal coefficient of linear correlation, not less than 0.9900, and then all the electrical parameters – burning voltage  $U_b$  and ignition parameters (voltage  $U_{ig}$  and current  $I_{ig}$ ) of the *DBDs* operating areas - first and next ones, have been calculated, [2].

## RESULTS AND DISCUSSION

The burning voltage  $U_b$  and ignition current  $I_{ig}$  calculated from discharge models, the real power  $P$  can be determined as a function of current  $I_{AVG}$  through the electrode configuration, or corresponding voltage drop  $U_{RMS}$  across the electrode cell, for all operating areas, [for  $(I_{AVG} - I_{ig, AVG}) > 0$ , or  $U_{RMS} > U_{ig, RMS}$ ], after the next equation (*Filippov-Emeljanov*, 1958), Fig. 2:

$$P = U_b (I_{AVG} - I_{ig, AVG}), \text{ W.} \quad (1)$$

The real specific power  $p_0$  (per one length of the high voltage electrode) is calculated from the real length of electrode configuration  $L = 0.130$  m, Fig. 3:

$$p_0 = \frac{P}{0.130}, \text{ W/m (Wpm).} \quad (2)$$

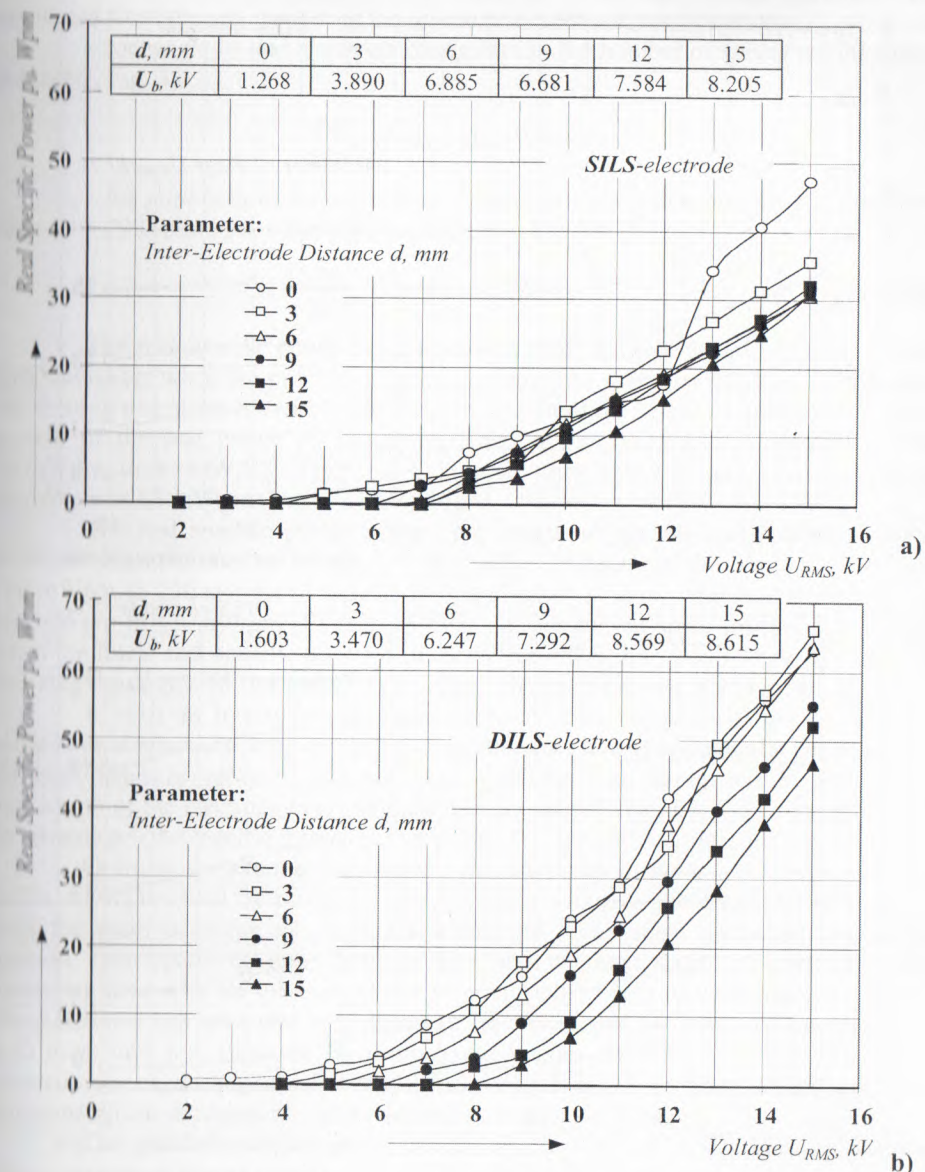
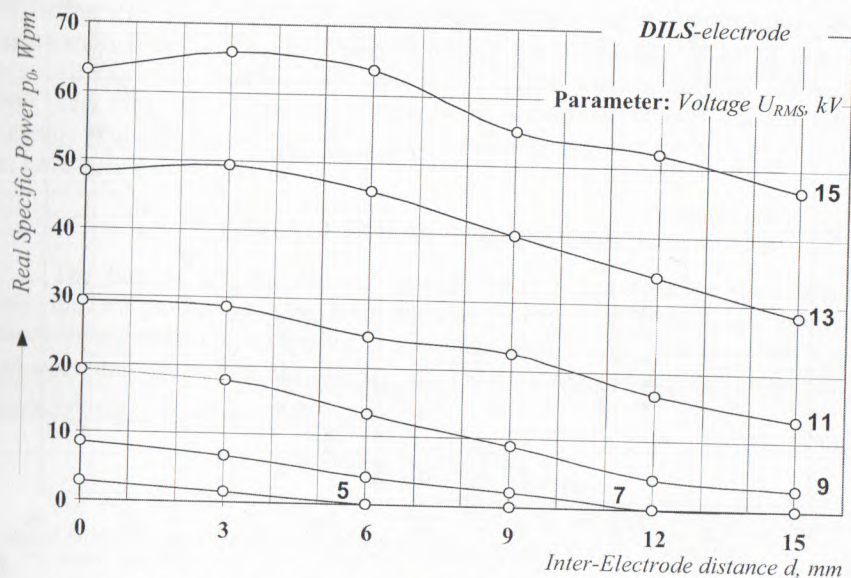
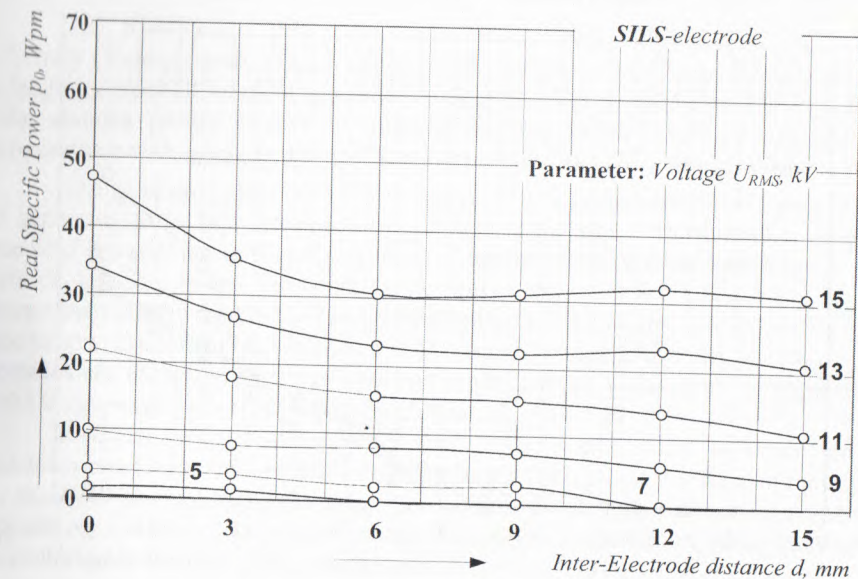


Figure 2. Families of energy efficiency characteristics of *pin-to-plate DBDs*  $p_0 = f(U_{RMS}), d = const.$ , with electrode configuration: **a** – *single-in-line* spikes (*SILS-*) electrode; **b** – *double-in-line* spikes (*DILS-*) electrode.



**Figure 3.** Families of energy efficiency characteristics of *pin-to-plane* DBDs:  $p_0 = \varphi(d)$ ,  $U_{RMS} = const$ , with electrode configuration: **a** – *single-in-line* spikes (SILS-) electrode; **b** – *double-in-line* spikes (DILS-) electrode.

The real specific power  $p_0$  (per one spike of the high voltage electrode) was calculated from the real number of the investigate electrode configuration:

- for *single-in-line electrode configuration* the number of spikes is 200 spikes per meter, Fig. 3a:

$$p_s = \frac{p_0}{200}, \text{ W per spike (Wps);} \quad (3)$$

- for *double-in-line electrode configuration* the number of spikes is 400 (two rows with 200 spikes per meter) spikes per meter, Fig. 3b:

$$p_s = \frac{p_0}{400}, \text{ W per spike (Wps).} \quad (4)$$

The real specific power  $p_0$  (per one meter of electrode length) of *pin-to-plane* DBD increases when the number of spikes is double by adding a new row of spikes to the existing one at the distance of 20 mm (or four times the height of the spike). But the growth of the real power  $p_0$  is very different – for example, the growth is from 30 mWpm to 64 mWpm (6 mm, 15 kV); and other example: the growth is from 46 mWpm to 66 mWpm (3 mm, 15 kV), Fig. 3.

The real specific power  $p_s$  (per one spike) of *pin-to-plane* DBD in general decrease when the number of spikes is doubled – for example, the diminution is from 180 mWpm to 130 mWpm (3 mm, 15 kV); and other example: the diminution is from 160 mWpm to 130 mWpm (12 mm, 15 kV), i. e. the current spike loading  $p_s$  decrease when the linear real specific power  $p_0$  increase by adding one parallel row of spikes or realizing the double-in-line spikes high voltage electrode *pin-to-plane*, Fig. 4.

It exist an interaction between the local spike microdischarges of adjacent spike lines at relatively large distances – four times the height of particular spike, for the different distances between electrodes, Fig. 4. If this examination will be applied for unit length of the electrode configuration (per one meter) then *DILS*-configurations has its advantage - the specific discharge real power  $P$  is higher with more then 50 %.

Ordinary the external volt-ampere characteristics of *plane-to-plane* (co-planar) DBDs are represented by polygonal linear models with tree sub-areas that correspond with the main development stages of discharges - the stage preceding the DBDs ignition, (non-operating area); and the first and the next stages of burning DBDs (operating area with its sub-areas). The external volt-ampere characteristics of *pin-to-plane* DBDs at low inter-electrode distances are represented by polygonal linear models with more then tree sub-area. By analogy, the energy efficiency or the technological characteristic of *pin-to-plane* DBDs  $p_0 = f(d)$  or  $p_s = \varphi(d)$ ,  $U_{RMS} = const$ , are presented by polygonal linear models with more than two operating sub-area.

The generalized real power model of *pin-to-plane* DBDs burning has the following special feature common for all DBD-based discharges:

i) the *pin-to-plane* DBD burns at a constant burning voltage, i. e.  $U_b = const$ , but the inter-electrode distance  $d$  does not significant influence on the change of the burning voltage and the real power  $P$ ;

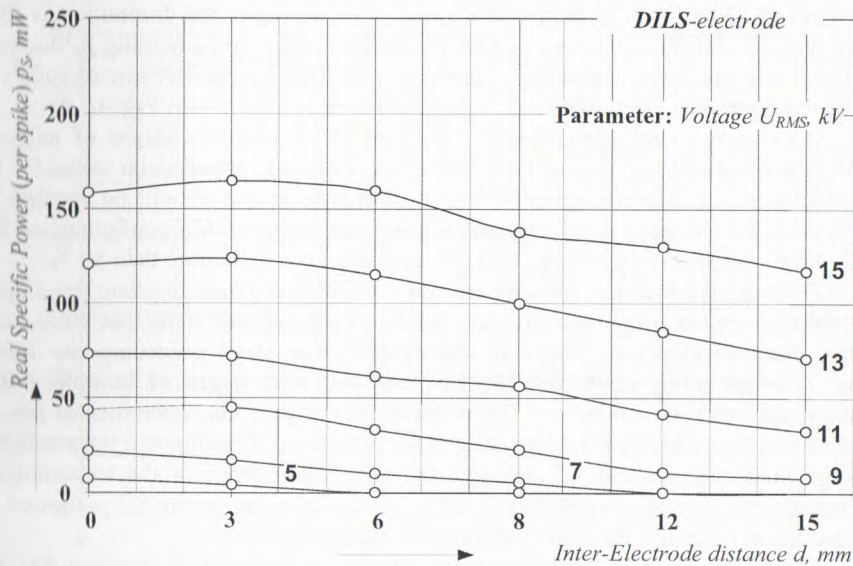
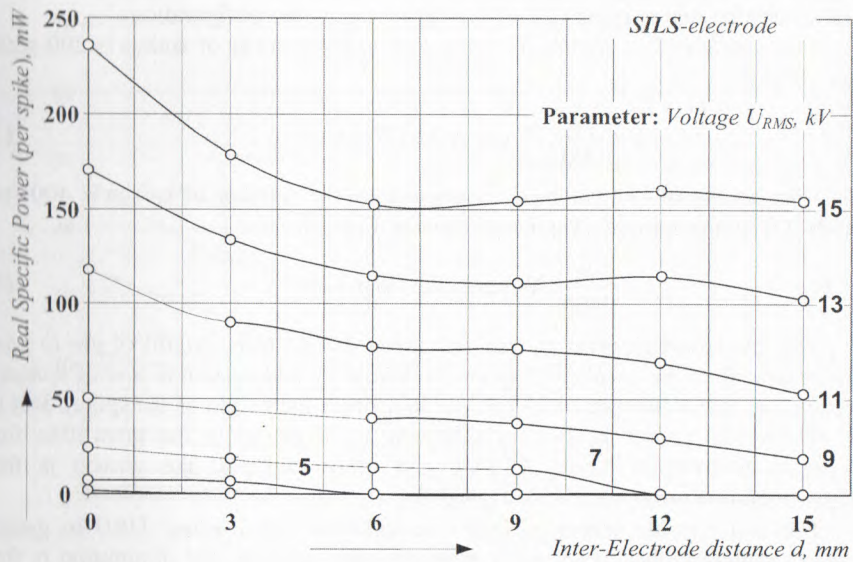


Figure 4. Families of technological pin-to-plane DBDs characteristics  $p_s = \varphi(d)$ ,  $U_{RMS} = const$ , of the two investigated electrode configurations: a – single-in-line spikes (SILS-) electrode; b – double-in-line spikes (DILS-) electrode.

ii) the ignition of pin-to-plane DBD or the transitions to a new operating area are threshold processes occurring for certain critical parameters – ignition voltages and currents ( $U_{ig}$  and  $I_{ig}$ ) – but the inter-electrode distance  $d$  does not significant influence on the change of the critical parameters  $U_{ig}$  and  $I_{ig}$  and the real power  $P$ ;

iii) the pin-to-plane DBD have to be described by the linear relationship between the real power  $P$  and the RMS value of voltage – the coefficient of linear correlation gets values above 0.9900 at low inter-electrode distances –  $d \in [3 \div 15 \text{ mm}]$  or  $d^* = d/L \in [0.6 \div 3.0]$ .

This model is based on following linear equation for all operating areas –  $P = D \cdot U_{RMS} + C$ , where  $D$  is the slope,  $W/V$ , and  $C$  – the intercept of the geometric line,  $W$ .

XPS- measurements have been used to study the resulting plasma-chemical modifications on the polymer surface. XPS analysis in this work was carried out using an photoelectron spectrometer VGS ESCALAB Mk II with Al  $K\alpha$  x-ray radiation ( $h\nu = 1486.6 \text{ eV}$ ;  $FWHM = 0.5 \text{ eV}$ ). XPS instrument use soft x-ray (200–2000 eV) radiation to examine core-levels. The angle between the incident X-ray directions and the observations (fixed by analyzer entrance slit) was  $50^\circ$ . Used instrument accept samples: 10 x 10 mm. The minimum analysis area ranges are from 10 to 200 micrometers ( $\mu\text{m}$ ).

XPS- analysis is a surface chemical analysis technique that can be used to analyze the surface chemistry of a material in its "as received" state, or after some treatment such as non-thermal plasma with pin-to-plane DBDs (only for one minute), for example. XPS detects all elements with an atomic number ( $Z$ ) of 3 (lithium) and above. This limitation means that it cannot be detect hydrogen ( $Z=1$ ) or helium ( $Z=2$ ). Detection limits for most of the elements are in the parts per thousand ranges (0.1 atom % = 1 part per thousand = 1000 ppm).

Table 1. XPS- surface chemical analysis of surface plasma-chemically treated heart wood samples.

X-ray photoelectron spectroscopy (mono-Al $K\alpha$ radiation)							
Douglas fir Wood Samples After DBD Plasma Treatment	Operational Voltage Area Above $U_b$ , kV	RMS Voltage $U_{RMS}$ , kV	Specific Real Power $P$ , Wpm <sup>2</sup>	Wood Surface Composition ( $1 \div 5 \text{ nm}$ usually), at. %			
				C	O	N	
Pin-to-plate DBD	No.1	7.0	201.900	76.5	23.4	0.1	
	No.2	6.628	9.5	855.400	83.0	16.8	0.2
	No.3	10.776	11.0	1230.000	84.9	14.6	0.5
Co-planar DBD	No.4	7.000	10.0	2.565	68.3	31.7	0.0
	No.5	11.920	15.0	56.037	69.1	29.9	1.0
K	No.6	-	-	-	77.7	21.8	0.5



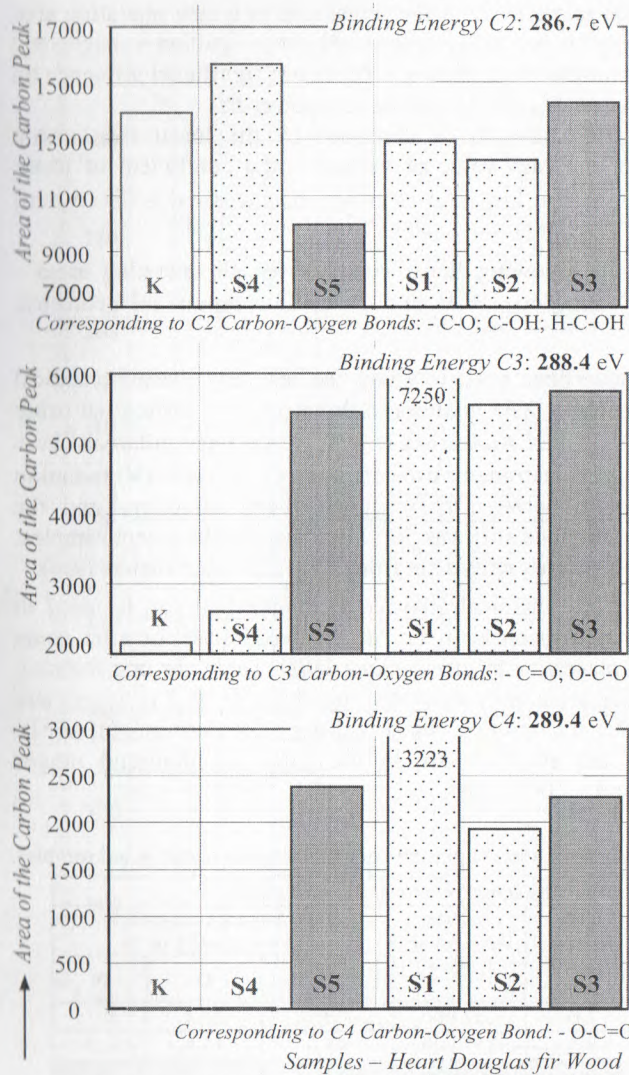


**Figure 5.** Carbon peak areas (in relative unit), or carbon-oxygen bonds quantity, of the typical for Douglas fir wood carbon peaks after Kazayawoko, 1998.

The presence of peaks at particular energies indicates the presence of a specific element in the sample under study - furthermore, the intensity of the peaks or the area under the peaks is related to the concentration of the element within the sampled region. Thus, the technique provides a quantitative analysis of the surface composition and in sometimes known by the alternative acronym, ESCA (Electron spectroscopy for chemical analysis).

Atoms of a higher positive oxidation state exhibit a higher binding energy due to the extra coulombic interaction between the photo-emitted electron and the ion core, Fig. 5.

This ability to discriminate between different oxidation states and chemical environments is one of the major strengths of the XPS technique.

As a result of the XPS measurements investigations the following main

conclusions can be derived: i) the quantitative analysis of the surface composition shows that the main result of the plasma-chemical surface interaction is expressed by the different oxidation states C2, C3 and C4 of carbon; ii) the behavior of the *co-planar* DBD

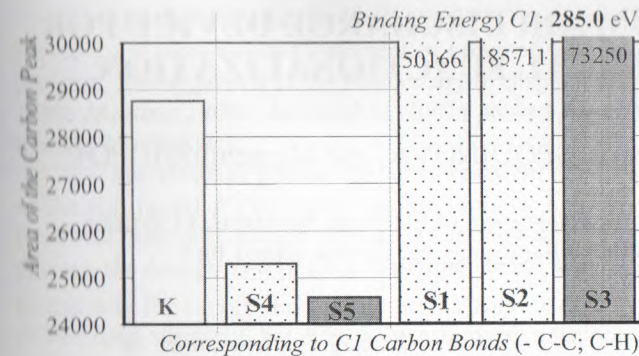


**Figure 6.** Carbon peak Cs1 area (in relative unit), or carbon bonds quantity, of the typical for Douglas fir wood carbon peak after Kazayawoko, 1998

cellulose and the wood, Fig. 5; iii) the *pin-to-pin* DBD has also two operating area – the first one from 6.628 to 10.776 kV, and the second – above 10.776 kV, but there is not predominant carbon-oxygen bonds – there are single, double and O-C=O bonds on the surface together, Fig. 5; iv) it is possible to suppose that the *pin-to-plane* DBD create C-H bonds on the surface while the *co-planar* DBD sharply diminish the quantity of C-H and C-C bonds.

## CONCLUSIONS

The present research formulates the problem of the pin-to-plane electrode configuration or the influence of the local non-uniformity of electrical field on the elementary processes in cold non-equilibrium plasmas, external electric characteristics and energy efficiency parameters. The *pins-to-plane* DBDs burns in every operating sub-area at constant burning voltages  $U_b$ , and the real power  $P$  is a linear function of RMS voltage drop across the electrodes. The linear functional subordination between the real power and RMS voltage is a distinguishing feature for all the DBDs. The *pins-to-plane* DBDs with higher energy suggest the through likely oxidation states of carbon at 286.7, 288.4 and 289.4 eV. It is one new different but very effective instrument for surface functionalization (oxidation) of wood (Douglas fir).

## REFERENCES

- [1] Dineff, P., Gospodinova, D., Kostova, L., Vladkova, T., and Chen, E.: Plasma aided surface technology for modification of materials referred to fire protection. Problems of Atomic Science and Technology, 2008, 6; Series Plasma Physics (14), pp. 198-200.
- [2] Dineff, P., D. Gospodinova. Electrode Configuration and Non-Uniform Dielectric Barrier Discharge Properties. XVI-th International Symposium on Electrical Apparatus and Technologies "SIELA 2009", 04-06 June 2009, Bourgas, Bulgaria; Proceedings, 2009, vol. 1, pp. 79-88.

# NON-EQUILIBRIUM AIR DISCHARGE DEVICE FOR PLASMA-CHEMICAL FUNCTIONALIZATION

Peter DINEFF, Dilyana GOSPODINOVA, and Momchil SHOPOV

Technical University of Sofia, Department of Electrical Apparatus, 1156 Sofia, Bulgaria, E-mail: [dineff\\_pd@abv.bg](mailto:dineff_pd@abv.bg); [dilianang@abv.bg](mailto:dilianang@abv.bg)

**Abstract.** New types of AC dielectric barrier discharges in ambient air (at atmospheric pressure and room temperature) for plasma-chemical functionalization of low-energy surfaces were investigated. A combination between dielectric barrier discharge (DBD) at low (in vacuum), and high (atmospheric) pressure, was sustained in an electrode configuration combining electrode components of both – spiral electrode into a quartz (dielectric barrier) tube under low pressure in argon, and second spiral electrode outside tube in ambient air. It was investigated experimentally the burning behavior of this low-high pressure DBD. The low-high pressure DBD behavior under different pressure in so called vacuum electrode (argon) was discussed.

**Keywords:** burning voltage, critical parameters of ignition, dielectric barrier discharge, and low-high pressure dielectric barrier discharge.

## INTRODUCTION

Low-temperature non-equilibrium plasmas are effective tools for surface treatment of various materials in micro-electronics, manufacturing and other modern industrial applications. The plasma-chemical surface influence of atmospheric pressure discharge presents advantages such as plasma treatment with cheap gas mixture or air, low specific energy consumption and short processing time.

Functionalization leads to formation of functional groups on the surface by chemical reaction between gas-phase species (Chan, 1994). Functionalization change, but mostly improves the wettability, the adhesion, lamination to other film, the printability and other coating applications, the capillary activity and impregnation of porous media (Dineff, 2004). In reality these different processes are not strongly separated, e.g. functionalization may include cleaning and sputtering. The depth scale of different processes are as follows: etching – 10÷100 nm; functionalization – 1÷5 nm, and coating – 10÷1 000 nm (Behnisch, 1994). The efficiency of various plasma components in surface functionalization is very different: ions and neutrals (kinetic energy: ~ 10 eV) components that cause chemical interactions in depth (monolayer); reactive neutrals (thermal energy: 0.05 eV) – chemical surface reactions and functional groups formation (depth: monolayer); electrons (kinetic energy: 5÷10 eV) – surface ionization and dissociation (depth: ~ 1 nm); photons (VUV: > 5 eV; UV: < 5 eV) – photochemical and secondary processes (depth: micron range).

The dielectric barrier discharge (DBD) seems to be the most promising plasma source for plasma-assisted treatment of polymer (and wooden) surfaces at atmospheric pressure. Investigations of the filamentary or disperse DBD (Behnke, 1996; Dineff et al, 1999; Massines, 2001; Sonnenfeld, 2001) proved the applicability of DBD for surface treatment techniques.

The effect of plasma chemical treatment depends on the real energy  $E$  (W sek) or the real power  $P$  (W) input into the process:  $E = P t$ , where  $t$  is the duration of the treatment, sek. For energy flow on an immobile substrate immersed in the discharge plasma, the dosage  $D = (P t) / A$  was used, J/cm<sup>2</sup>, where  $A$  is the electrode surface, cm<sup>2</sup>. In this way for energy flow on the barrier surface of a surface DBD, fig. 2a, the dosage  $D$  was used similarly, but  $A$  is the quartz barrier surface. The dosage is proportional to real power  $P$ . The real power is an important parameter of DBD to achieve desired surface chemistry or the quantity of gaseous product.

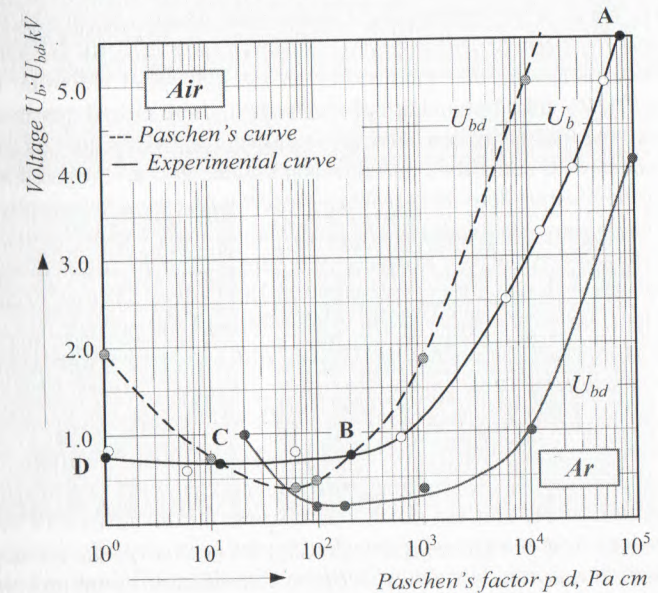


**Figure 1.** Burning voltage  $U_b$  of AC DBD in coplanar electrode configuration at electrode distance 0.6 cm and compensated edge effect as a function of pressure  $p$ , and Paschen's law (curve) for DC breakdown voltage  $U_{bd}$  in dry air, where  $p$  is the pressure, Pa;  $d$  – distance between electrodes, cm.

Special applications of DBD under low pressure (in vacuum) exist – the burning voltage drop across the inter-electrode gap is constant too during the discharge burning:  $U_b = const$ . The experimental results, presented by [1], enable as to show the burning voltage  $U_b$  of a DBD in coplanar electrode configuration as a function of the pressure, and to compare it with the breakdown voltage  $U_{bd}$  of dry air and argon (Ar), fig. 1.

The aim of this paper is the experimental investigation on the ignition and the burning behavior of a new type of AC DBD in ambient air at atmospheric pressure and room temperature for plasma-chemical functionalization of low-energy (polymeric) surfaces, fig. 3.

### LOW-HIGH PRESSURE DIELECTRIC BARRIER DISCHARGE

A combination between vacuum DBD burning at low pressure (under 1 000 mbar), and atmospheric DBD burning under high pressure, was sustained in an electrode configuration combining electrode components of both – spiral electrode into a quartz tube (quartz dielectric barrier) was immersed in argon under low pressure. Second spiral electrode was arranged on the tube surface immersed in ambient air. It experimentally was investigated the ignition and burning behavior of this low-high pressure DBD (LHP DBD). The LHP DBD behavior under different pressure in so called vacuum electrode (under argon) was discussed. We take the view that the LHP DBD is a combination of two serially powered DBDs that burn in co-axial cylindrical electrode configuration, Fig. 2c: the first DBD burns among the windings of an external spiral electrode in ambient air at atmospheric (high) pressure, Fig. 2a; the second DBD burns among the windings of an internal spiral electrode in argon under low pressure, fig. 2b. The internal spiral electrode and the closed quartz tube under low pressure constitute the so called tubular vacuum electrode, Figs. 2d and e. Vacuum tubular electrodes with straight electrode was produced and investigated too, Fig. 2f.

Surface plasma activation (SPA) device with one surface-plasma activation applicator was produced for Shenjang institute of chemical technology (Liaoning, China) and was investigated, Fig. 2g. The applicator holds two vacuum tubular electrode powered on  $U_{pk} = 7$  kV at 30 kHz, fig. 2h.

Vacuum tubular electrodes under different low-pressure have been made purposely for this project by European Lighting Industry Ltd., Sliven, Bulgaria.

### EXPERIMENTAL INVESTIGATION

The atmospheric low frequency DBD electrode configuration consists of two cylindrical co-axial electrodes separated by a dielectric barrier – the internal electrode is made as a metallic tube, and the other – as a spiral on the surface of the quartz tube, Fig. 2a. The edge effect is as usually detached by the geometry of electrodes.

The vacuum low frequency DBD electrode configuration consists of two cylindrical co-axial electrodes separated by a dielectric barrier - the internal electrode is made as a spiral on the inside surface of the tube, and the external – as a metallic tube, Fig. 2b. The combined low-high pressure DBD electrode configuration consists of two cylindrical co-axial spiral electrodes arranged at the two side of the quartz tube - internal and external, Fig. 2c.

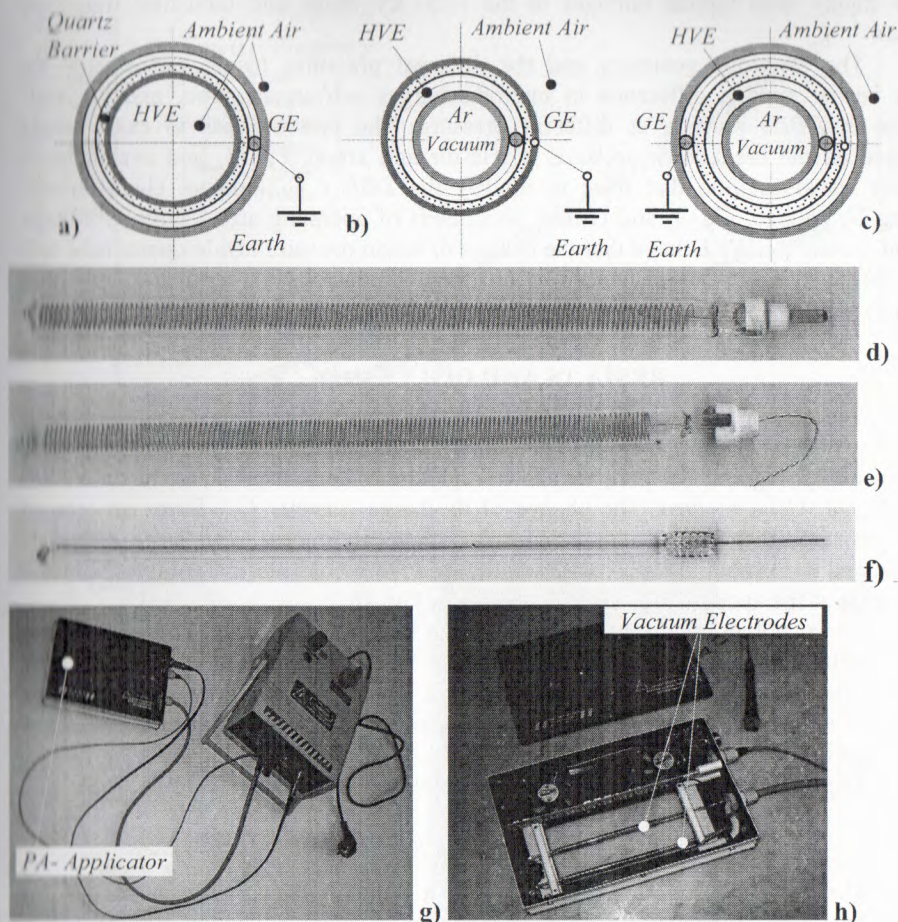


**Figure 2.** Schematic of the electrode configurations of low-high pressure dielectric barrier discharges: **a** – typical co-axial cylindrical electrode configuration of dielectric barrier discharge (DBD) with external spiral earthed electrode at high (atmospheric) pressure; **b** – co-axial cylindrical electrode configuration of DBD with internal spiral electrode at low (in vacuum) pressure; **c** – combined low and high pressure DBD with vacuum tubular electrode; **d** and **e** – vacuum tubular electrodes including an internal spiral metal electrode and a tubular quartz barrier under vacuum inside; **f** - vacuum tubular electrode with straight internal metal electrode; **g** – surface plasma activation (SPA) device with surface plasma activation applicator, made for Shenjang Institute of Chemical Technology, Liaoning, China; **h** – plasma activation applicator (PAA) with two vacuum electrodes. Vacuum electrodes have been made purposely for this project by European Lighting Industry, Ltd., Sliven, Bulgaria.

The dielectric tube is filled with argon under low pressure. The pressure range is: 1, 100, 200, 400, 800, and 900 mbar. The electrodes are energized by a high voltage

power supply with typical voltages in the 1÷20 kV range and industrial frequency (50 Hz).

The electrode geometry and the different pressures inside and outside the quartz barrier need a difference in microdischarges self-organization, and “crystal” patterns in DBDs burning at different pressure. The pressure has to exert strong influence on the breakdown voltages  $U_{bd}$  in air and argon, Fig. 1, and avalanche to streamer transformation that have to modify the DBD’s volt-ampere characteristic, burning  $U_b$  voltage, Fig. 1, and critical parameters of operating area - ignition voltage  $U_{ig}$  and current  $I_{ig}$ . We believe that the change of argon pressure inside quartz tube will give rise to the typical influence on electrical characteristics, critical or ignition parameters, and real power of LHP DBDs.

## RESULTS AND DISCUSSION

The static external, or volt-ampere, characteristics  $I_{AVG} = f(U_{RMS})$  of LHP DBDs for different argon pressure ( $p = const$ ) in the quartz tube have been plotted experimentally, Fig. 3a. The data are shown replotted as current-pressure characteristics  $I_{AVG} = f(p_{Ar})$ ,  $U_{RMS} = const$ . The change of discharge currents  $I_{AVG}$  forms an area of argon pressures that correspond to effective chemical process with large discharge currents and corresponding real power in the two DBD cold plasma volumes – inside and outside of the vacuum high voltage electrode, Fig. 3b.

Linear polygonal discharge models have been worked out in accordance with [2], for a minimal coefficient of linear correlation, not less than 0.9900, and then all the electrical parameters of the DBD operating areas have been calculated and figured as function of argon pressure – burning voltage  $U_{b, RMS}$ , Fig. 4, ignition or critical voltage  $U_{ig, RMS}$ , and ignition current  $I_{ig, AVG}$ , Fig. 5.

The real power of LHP DBDs is given by (Filippov and Emelianov, 1958):

$$P = U_{b, RMS} (I_{AVG} - I_{ig, AVG}).$$

The real power  $P$  was figured as a function of argon pressure  $p$  at  $U_{RMS} = const$ . An interesting for the plasma-chemical functionalization area of power efficiency was formulated between 400 and 800 mbar: the real power  $P$  in this interval of argon pressure is higher - more two times above, than other pressures, Fig. 6.

From an operational viewpoint, the higher real power  $P$  correspond to higher discharge current  $I_{AVG}$ , or the high real powers require high discharge currents. No other DBD configuration studied to date shows such a behavior – most DBD configurations studied show that the burning voltage  $U_{b, RMS}$  and the ignition current  $I_{ig, AVG}$  have the important influence on real power  $P$ . Figures 4a and 5b show weak burning voltage and ignition current deviations as a function of argon pressure for a large interval of pressure change. The change of argon pressure  $p$  in the vacuum high voltage electrode has not significant influence on the burning voltage and the ignition parameters of LHP DBD but it increases the real power  $P$  by increasing the discharge current  $I_{AVG}$ , Figs 3b and 6.

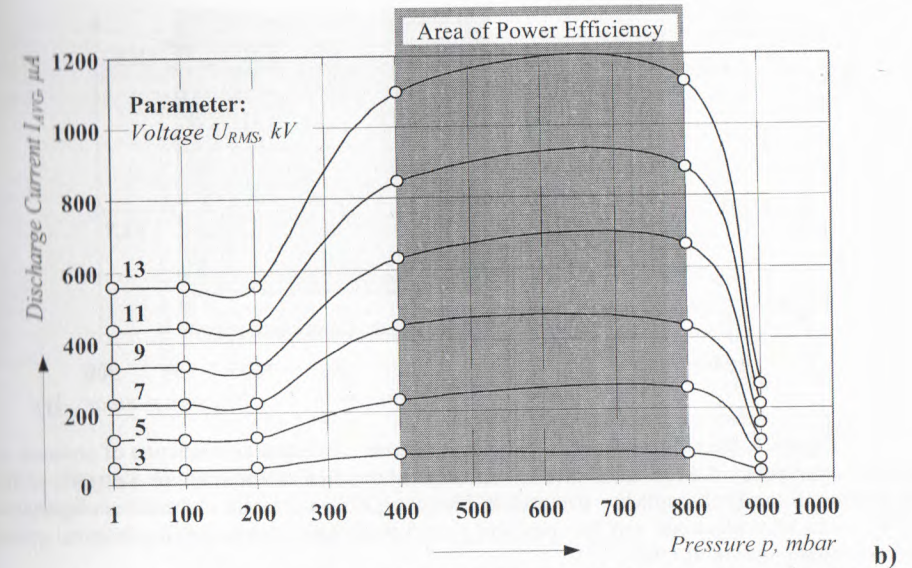
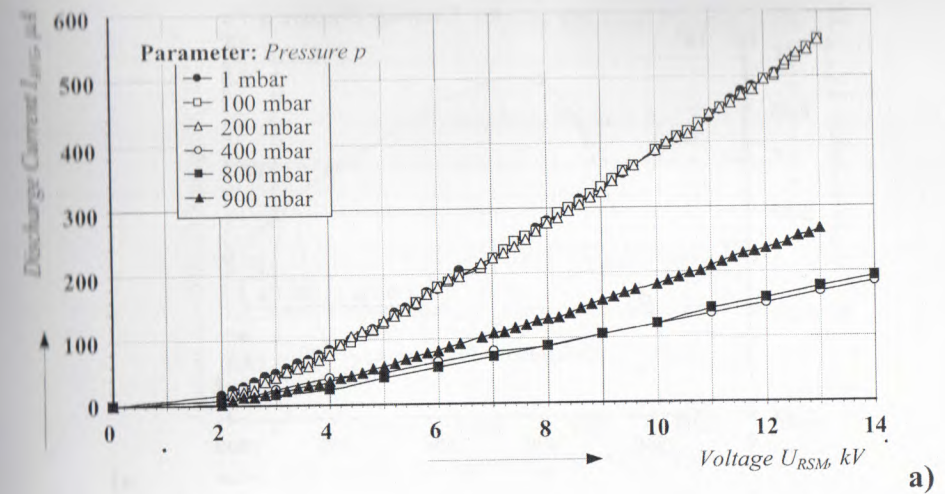


**Figure 3.** Statical volt-ampere characteristic  $I_{AVG} = f(U_{RMS})$ ,  $p = const$  (a) of co-axial cylindrical spiral electrode configuration of DBD with vacuum electrode under low pressure  $p$  inside (argon), and ampere-pressure characteristic  $I_{AVG} = \varphi(p)$ ,  $U_{RMS} = const$  (b). The area of power efficiency presents conditions for capacity real power.

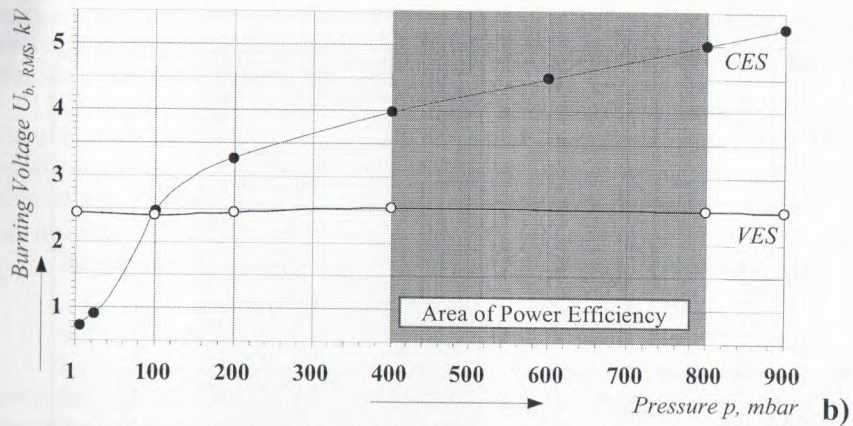
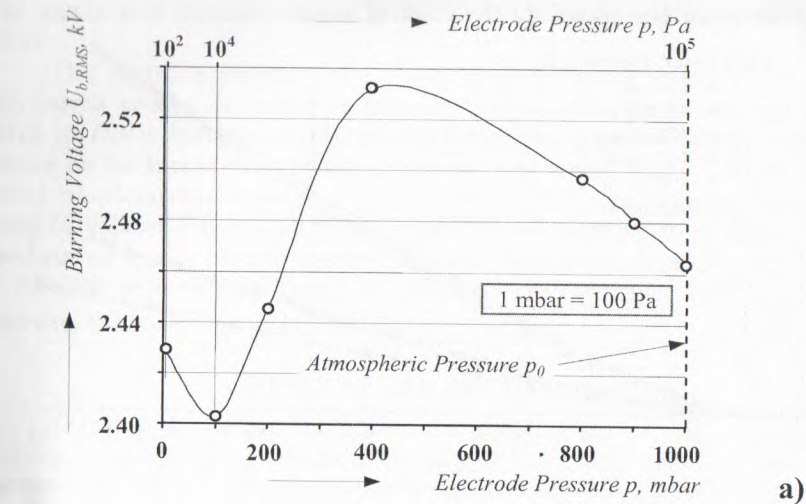


**Figure 4.** Burning voltage  $U_b$  of dielectric barrier discharge as a function of pressure  $p$ : **a** - VES – co-axial cylindrical spiral electrode configuration of DBD with vacuum electrode under low pressure  $p$  inside (argon); **b** – comparison between CES – co-planar electrode configuration of DBD with inter-electrode gap low pressure  $p$  (air) and VES – the co-axial cylindrical spiral electrode configuration of DBD.

In order to characterize the increasing of real power of LHV DBD, a supposition was suggested: the DBD in argon under low pressure plays the leading part as an efficient UV-radiation source for the going ionizing and chemical processes in atmospheric plasma, and the atmospheric DBD plays the same part for the going ionizing and chemical processes in vacuum non-equilibrium and non-thermal plasma. If the pressure of argon in vacuum tube is varied the UV-radiation across the quartz tube exert influence on the going ionizing and chemical processes in atmospheric plasma: the manifestation of this influence was studied experimentally.

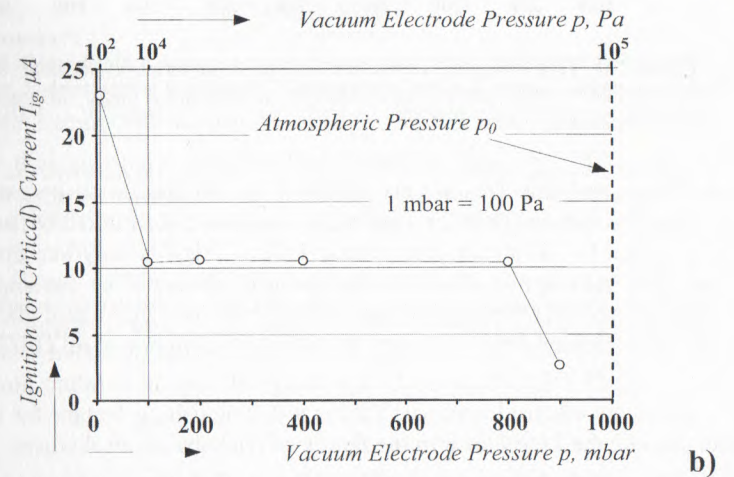
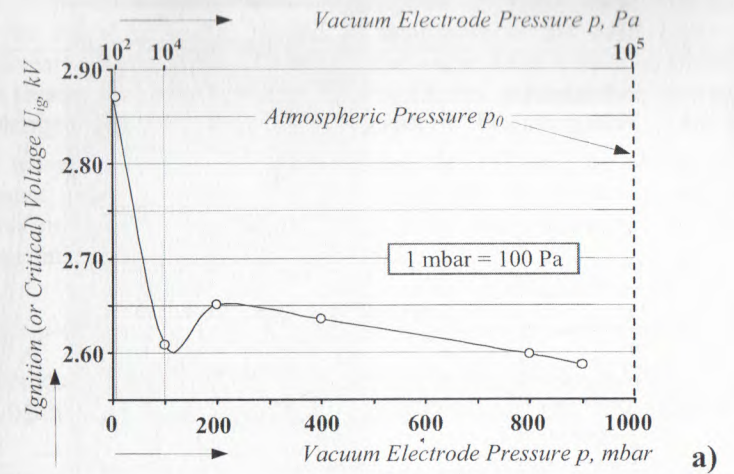


**Figure 5.** Ignition (or critical) parameters of a co-axial cylindrical spiral electrode configuration of DBD: **a** – ignition voltage  $U_{ig}$  of DBD; and **b** – ignition discharge current  $I_{ig}$  of DBD as a function of pressure  $p$  (argon).

## CONCLUSIONS

As a result of the experimental investigations of LHP DBD with co-axial spiral electrodes, the following main conclusions can be derived:

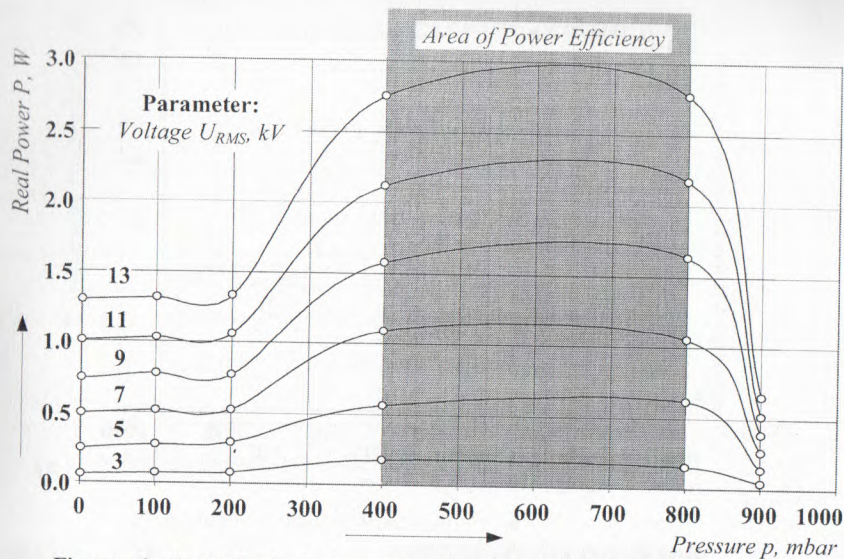


**Figure 6.** Technological characteristics of a co-axial cylindrical spiral electrode configuration of DBD – real power  $P$  as a function of pressure  $p$  under different voltage drops  $U_{RMS}$  across the electrode system, and area of power efficiency of DBD surface functionalization.

- The LHP DBD with electrode configuration containing is a typical DBD-based discharge and this fact is very good shown by the linear operational law for  $I_{AVG} = f(U_{RMS}), p = const$ . But the operating area is not constituted by more operating sub-areas, typical for co-planar atmospheric DBDs. There is only one operational area producing cold non-equilibrium and non-thermal plasma. The assumption that the combination of two DBDs energized and burning in serial DBD-based discharge is fully acceptable as a common DBD with properties that are common to all DBD;

- The LHP DBDs burn in the operating sub-area at constant burning voltages drop  $U_b$  across the electrode system. This is a distinguishing feature for all the DBDs. That fact put also the LHP DBDs in the family of DBD-based discharges;

- The specific behaviour of LHP DBD is well shown at different argon pressure in vacuum high-voltage electrode. The real power increases in the low pressure interval from 400 to 800 mbar following the change of discharge current. The change of argon pressure in the vacuum electrode has not significant influence on the burning voltage and the ignition parameters of LHP DBD. That's probably the effect of vacuum DBD UV- irradiation influence on atmospheric DBD across the quartz (dielectric) tube and vice versa.

- The LHP DBD created by the use of a specific vacuum high voltage electrode filled with argon under low pressure is a good technical decision because it suggests better discharge energy efficiency – higher discharge current and real power, and higher dosage of energy flow;

- The method of mathematical description of DBD static volt-ampere characteristics by linear polygonal models is applicable to the LHP DBDs. The coefficient of linear correlation gains values about unity: from 0.9978 to 0.9985 for different argon pressure. There is a strong linear functional subordination between the average of discharge currents and the RMS of voltages;

- The present experimental research formulates the problem of the vacuum electrode pressure (argon) influence on the elementary processes in cold non-equilibrium and non-thermal plasmas, external electric characteristics and power efficiency parameters.

## ACKNOWLEDGEMENT

The financial support of the National Science Fund, Ministry of Education and Science of Bulgaria, for the Research Project DO-02-11: EF/2009 is gratefully acknowledged.

## REFERENCES

- [1] Dineff, P., D. Gospodinova. *Characteristics and Behaviors of Dielectric Barrier Discharge at Different Air Pressure*. V. International Conference "Challenges in Higher Education and Research in the 21-st Century "CHER-21'07", June 01-04, 2007, Sozopol, Bulgaria. Proceedings of full papers, 2007, pp. 273+276.
- [2] Dineff P., D. Gospodinova. *Electric Characteristics of Dielectric Barrier Discharge*. XXXVI. International Scientific Conference on Information, Communication and Energy Systems and Technologies "ICEST '2003", Sofia, Bulgaria, 16-18 October, 2003. Proceedings of full papers, Heron Press., Ltd., Sofia, 2003, pp. 442+445.
- [3] Pal, U., M. Kumar, H. Khatun and A. Sharma. *Discharge Characteristics of Dielectric Barrier Discharge based VUV/UV Sources*. International Symposium on "Vacuum Science and Technology" (IVS 2007), Journal of Physics: Conference Series 114 (2008) 012065, IOP Publishing, doi: 10.1088/1742-6596/114/1/012065.